Validation of geometrical room acoustics algorithms by comparing predicted and measured room responses

A. T. Fürjes [*], É. Arató-Borsi [**], T. Póth [**] and F. Augusztinovicz [*]

[*] Technical University of Budapest, [**] Hungarian Radio, Budapest, Hungary, andor@sch.bme.hu

Abstract

Geometrical room acoustics modeling techniques are generally used in room acoustics when predicting the sound field in large spaces such as opera houses, theaters or concert halls. Well controlled sound field is probably more important and critical in reference listening rooms and recording rooms. Unfortunately, these are small in the acoustic sense, special materials and structures are applied and the effect of furniture and equipment is not negligible. Neither purely geometrical room acoustics algorithms nor traditional finite element techniques can be used effectively, the one being a very coarse approach and the other requiring very high computational efforts.

A series of modeling has been carried out by using various geometrical approaches, and the predicted room responses were compared to actual measurements. The goal of these investigations is to find a high and medium frequency modeling algorithm that predicts most important sound field parameters accurately enough.

1. Introduction

In practice, the properties of the sound field in rooms are generally modeled using algorithms based on the laws of geometrical room acoustics. These are proved to be reliable enough where the modeled room is not small in the acoustic sense, i.e. the linear sizes of obstacles found in the room are much larger than the wavelength at the frequencies in question [1].

However, there are cases where this condition is not fulfilled, so other modeling methods, for example finite element modeling must be used. Unfortunately while designing room acoustics, because of the computationally intensive algorithms, the use of numerical methods is worth in special cases or at extreme low frequencies only.

To study the validity of methods based on geometrical acoustics, a series of modeling and measurement has been carried out. Because they are typically small, special structures and materials are applied in them, and the quality of the sound field is more critical, control rooms and reference listening rooms in the Hungarian radio were chosen for this experiment.

This paper gives a short summary on geometrical room acoustics algorithms, shows theoretical possibilities for improving the validity of these methods, and finally reports the results of the experiments.

2. Geometrical room acoustics algorithms - a summary

In geometrical room acoustics the simple idealization of a sound ray is used rather than the concept of a wave. The sound ray is a small portion of the spherical wave front originating from the sound source, propagates in straight lines with the velocity of sound on a straight line and reflects optically [2]. From these postulates different algorithms have been developed.

2.1. Mirror image source method

If the room geometry is described with plane reflecting surfaces, the resulting sound field is described as a sum of the sound fields coming from virtual sources, where the positions of the virtual sources are the mirrored positions of the original sound source (Fig.1).

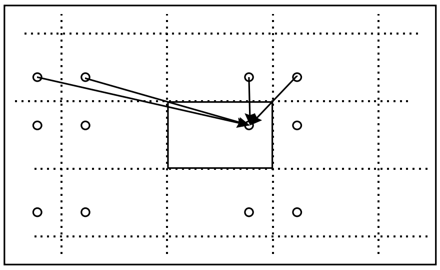

Figure 1. Mirror image source method

Limitations of this method are that the number of virtual sources is increasing exponentially with time and that the visibility of virtual sources has to be examined. Nevertheless, because of its precision, modeling algorithms often utilize this method for the first reflections until a given reflection order.

2.2. Ray-tracing method

The ray-tracing method uses a given number of sound particles to describe the wave front. All sound particles, called rays, have their own velocity, intensity and direction. The particles reflect from surfaces optically and are detected with a receiver surface (Fig.2) which is often a sphere around the receiver point.

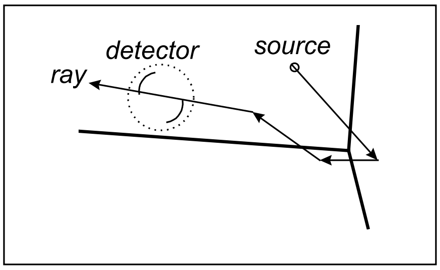

Figure 2. Ray-tracing method

Advantage of this method is the simple algorithm, but the detection process gives imprecise detection timing of reflections since results are in the form of a histeresis, which makes the evaluation sometimes more difficult [3].

2.3. Cone-tracing method

To have an exact intersection with a receiver point, instead of the particles, spherical cones are used to describe the wave front (Fig.3). This method combines the advantages of the mirror image source and the ray-tracing methods. However to solve the problem of the overlapping cone surfaces, a correcting weighting function must be used for each cone.

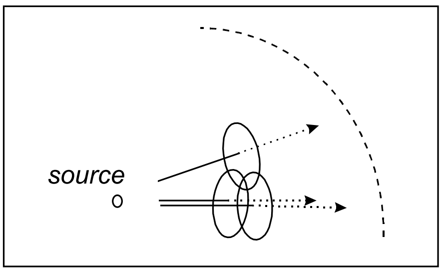

Figure 3. Cone-tracing method

2.4. Triangular beam-tracing method

Triangular beam-tracing methods don't suffer from the overlapping problem of the cone-tracing algorithms, because the wave front is described exactly by triangular pieces of the sphere (Fig.4).

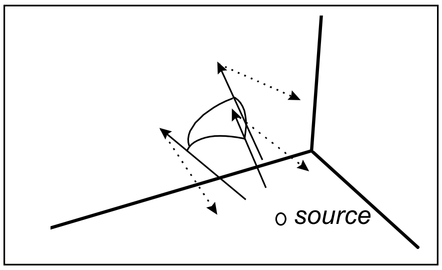

Figure 4. Triangular beam-tracing method

2.5. Sampled beam-tracing

This method uses the simple beam-tracing method, but because of the sampled examination of reflections, beams reflect only if they hit an obstacle larger than the wavelength of the given frequency [4] (Fig.5).

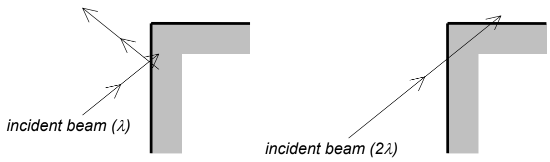

Figure 5. Sampled beam-tracing

Disadvantage of this model is that beam paths must be calculated for each frequency (wavelength).

2.6. Extensions of the geometrical methods

There are a number of wave propagation phenomena that pure geometrical acoustics methods cannot model. These are diffuse reflection, diffraction and refraction. The latter phenomenon is negligible in rooms, although environmental applications may need this feature.

Phase effects may be taken into account also assuming that sources are coherent and that the system is causal and linear thus phase responses can be calculated from amplitude responses [1].

2.6.1. Diffuse reflections

Diffuse reflection occurs, independently on the incidence angle, whenever the reflecting surface features irregularities - and this is almost always the case.

Diffuse reflections originate from the reflected energy and may be characterized macroscopically by defining a diffusion factor δ, so the equation for the absorbed, diffused and specularly reflected energy is using δ is [5]:

$$\underbrace{\alpha}_{absorbed} + \underbrace{\delta(1-\alpha)}_{diffused} + \underbrace{(1-\alpha)(1-\delta)}_{specular} = 1 \qquad (1)$$

where α is the absorption coefficient.

There are several methods for modeling diffuse reflections, but only few is able to handle diffuse to specular or diffuse to diffuse reflection combinations (Fig.6).

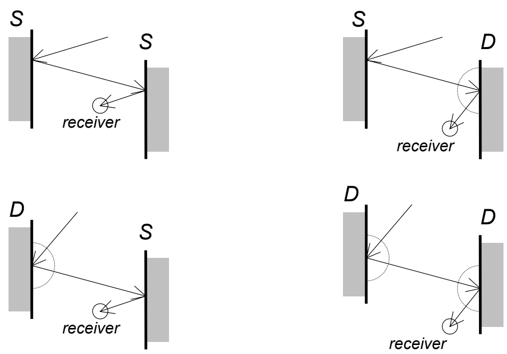

Figure 6. Different reflection combinations

2.6.2. Diffraction

Diffraction occurs around edges, so receivers in shadow-zones can detect energy, too. This phenomenon may be described accurately by finite element analysis. However, geometrical methods usually make use of approximative equations to calculate attenuation behind selected edges [6].

Another approach calculates diffraction as diffuse reflection if the surface is hit near an edge.

3. Validation process

It is obvious that the modeling techniques outlined above are only coarse approximations of the real phenomenon thus the validity of these methods must be examined. Therefore after measuring several rooms and comparing the objective and subjective result to determine the most important types of parameters, these parameters were also calculated and compared from the models.

For the measurements we used the MLSSA system from DRA, for the modeling the RAYNOISE simulation software package from LMS, finally results were processed using MATLAB.

3.1. Statistical results

Statistical results were examined first. Using the absorption coefficients taken from tables, global reverberation times were compared.

Calculated and measured statistical reverberation times matched well. However, it can be seen how small difference is shown if we consider furniture in the rooms (Fig.7).

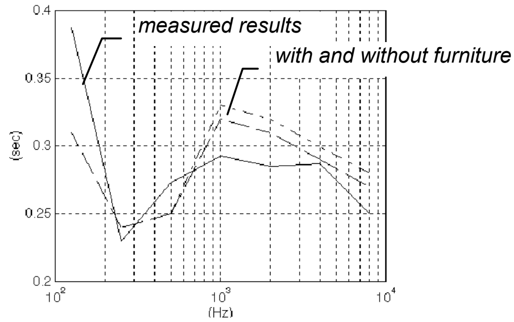

Figure 7. Statistical reverberation times (RT_{60})

3.2. Results at field points

It is evident that the furniture has a significant effect and that more detailed, position-dependent parameters are needed to describe the subjective quality of the sound field at each listening position.

For this reason several acoustical quantities were calculated from the measured impulse responses and compared with the modeled results at different field points.

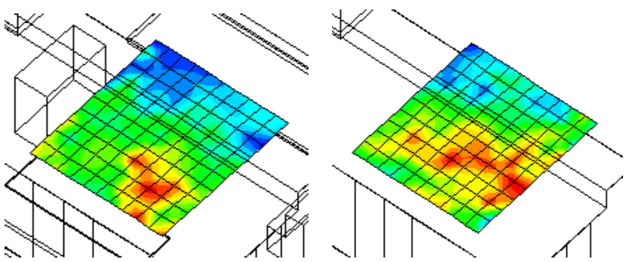

Figure 8. Central gravity time around the listening point, with and without furniture at 1000Hz

Examining different acoustical quantities and their change around the listening positions showed clear difference between the room with and without furniture, but the agreement between the measured and modeled results was not so trivial.

To inspect the causes of deviations the possible error sources had to be investigated.

3.3. Error sources of modeling

Our modeling experiences show, that errors during a modeling process are mostly due to the incomplete knowledge about the data describing the properties of materials. These include absorption coefficients, diffusion factors and their directionality.

Other error sources are the imprecise geometry description and/or source and receiver positions, their directional data, and last but not least, the limitations of the modeling method itself, of course.

In other words, if we assume that our geometrical room acoustics modeling algorithm is valid so that only the parameters are incomplete and incorrect, we have to study the effect of parameter errors on the modeling results.

Unfortunately we cannot discuss this parameter-sensitivity problem analitically because it largely depends on the geometry and the type of the algorithm itself. For this reason in the following part of this paper we assume the validity of the modeling process and study the parameter values only by comparing measured and modeled results.

3.4. Parameter calculation

If the modeling method is valid and parameters of the model are imprecise, we should calculate parameter values for the model in order to gain modeling results matching the measured ones.

Direct results from the modeling process are typically echograms showing the temporal distribution and the amplitudes of reflections from reflecting and diffusing surfaces around the receiver position at a given frequency (Fig.9).

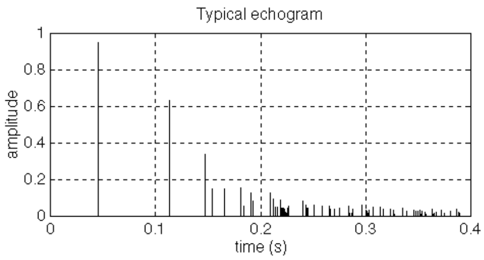

Figure 9. A typical echogram (e.g. at 1kHz)

Echograms also contain information about the history of a given reflection: what was the path of the reflection, which surfaces took part in the reflections, and so on.

The direct results from a measurement are usually wide-band impulse responses (Fig.10).

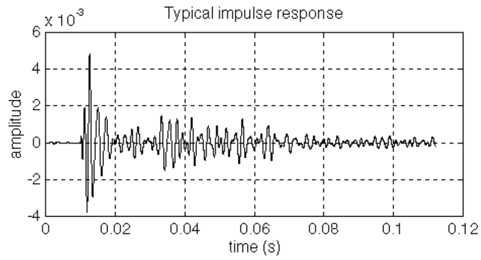

Figure 10. A typical room impulse response

As we can see, it is rather difficult if not impossible to fit monochromatic echograms to wide-band impulse responses directly in order to calculate the required parameters. Even if we calculate wide-band impulse responses from the echograms based on the assumption that the linear system of the room is causal, in practice the resulting ‘continuous’ time-domain impulse responses differ too much, mainly because of the lack of exact simulation of the phase relations.

Therefore the fitting process should be based on energy-time functions. Note, that this is reasonable also, since the reverberation quantities and most of the acoustic quality factors (Clarity, Definition, etc.) are based on energy-time integrals and ratios.

3.4.1. ETC fitting

For the fitting process the energy-time curve (ETC) is chosen:

$$\mathrm{ETC}(t) = 1 - \frac{\int_0^t p^2(t)\,dt}{\int_0^\infty p^2(t)\,dt} \tag{2}$$

where p(t) is the pressure at the receiver point (microphone). Instead of the ∞ usually the constant of 1sec is chosen because of the noise problems during the measurement.

The fitting is based on the information of the time intervals of incoming reflections (model-echogram) and the energy content ratios of the successive reflections (measured ETC).

The result is an echogram with the same timing as the modeled one and with the same energy decaying properties as the measured one (Fig.11).

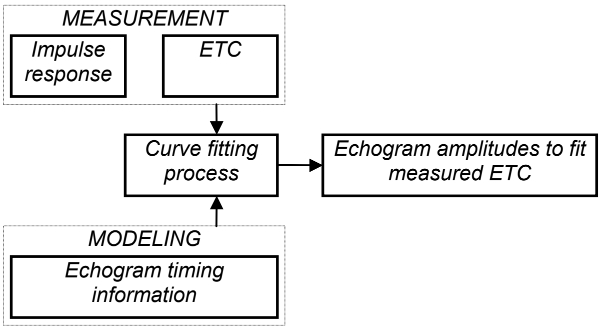

Figure 11. ETC fitting

In order to discuss the process we introduce a number of simplifications:

- the sources and receivers are supposed to be omnidirectional;
- diffuse reflections are neglected because they make the ETCs just smoother, but they don't affect their decay slope much, although they are subjectively preferable;
- we are interested only in the absorption coefficients
- geometry and positions are supposed to be exact.

For the experiments a well documented reference listening room in the Hungarian Radio was chosen (Fig. 12) having sound sources with fairly smooth and even directional characteristics and with very good transient response.

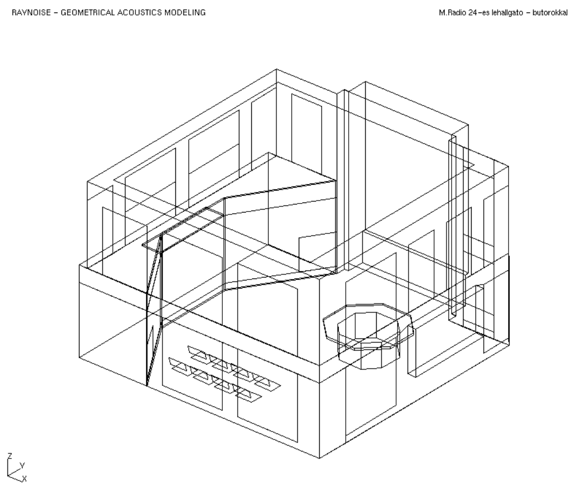

Figure 12. Geometry of the room

3.4.2. Calculating parameters from echogram

Generally spoken, if we assume the validity of the algorithm, with a point-like source and a receiver, where directivity is not taken into account, the receiver point detects the sum of reflections, where each reflection path has it own response function:

$$H_{rec}(\omega) = H_{src}(\omega) \cdot \sum_{i=1}^{\infty} H_{path,i}(\omega) \cdot \frac{e^{-j\omega t_i}}{c(\omega) t_i} \quad (3)$$

where H_{rec} is the resulting response function at the receiver position, H_{src} is the response function of the source, t_i is the time (length) of the reflection path, c is the propagation speed and $H_{path,i}$ is the response function of the i-th path:

$$H_{path,i}(\omega) = H_{air,i}(\omega) \cdot \prod_{n=1}^{N} H_{surf,i,n}(\omega) \quad (4)$$

where $H_{path,\ i}$ is for the air absorption, finally $H_{surf,i,n}$ is the response function of the n-th reflecting surface on the i-th reflection path.

After correcting the amplitudes of the reflections due to the air absorption, we may write the following equation system:

$$\begin{aligned} \prod_{n=1}^{N} H_{surf,1,n}(\omega) &= H_{path,1}(\omega) \\ &\vdots \\ \prod_{n=1}^{N} H_{surf,K,n}(\omega) &= H_{path,K}(\omega) \end{aligned} \quad (5)$$

For a given frequency in terms of energies:

$$\begin{aligned} (1-\alpha_1)^{M_{1,1}} \cdot (1-\alpha_2)^{M_{1,2}} \ldots (1-\alpha_N)^{M_{1,N}} &= E_1 \\ &\vdots \\ (1-\alpha_1)^{M_{K,1}} \cdot (1-\alpha_2)^{M_{K,2}} \ldots (1-\alpha_N)^{M_{K,N}} &= E_K \end{aligned} \quad (6)$$

where N is the number of surface types, α_n is the absorption coefficient of the n-th surface, E_i is the calculated and corrected energy of the i-th reflection of the echogram. Since a surface may take part in a reflection path more than once (or not at all), this multiplicity is expressed by $M_{i,n}$., which can be 0, 1, …, etc.

After taking the logarithm of Eq. (6), we get a simple linear equation system. A part of the coefficient matrix is shown 'from above' in Fig. 13.

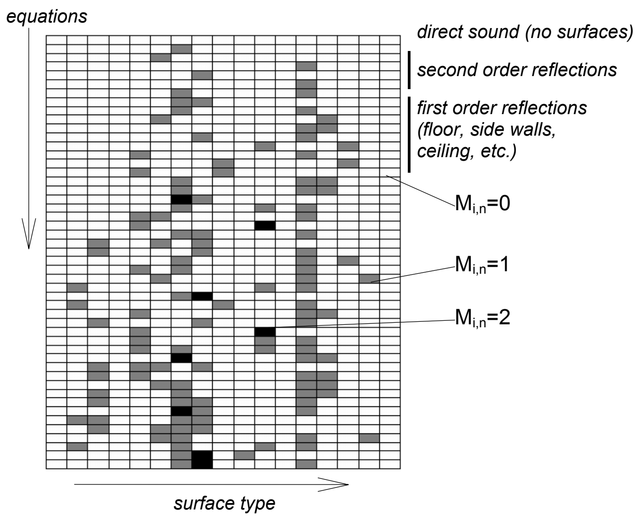

Figure 13. A part of the coefficient matrix

This equation system is strongly overdetermined, thus a special iterative procedure was created (Eq.6).

$$\overline{\alpha}_{k+1} = \overline{\alpha}_k + \gamma \cdot \overline{\delta}_k \qquad (6)$$

where the correction vector decays exponentially due to the coefficient γ, according to the following considerations:

- the first reflections are the most important,
- the decay slope of the ETC is important,
- the later part of the measured ETC is not as important because of noise problems during the measurement.

The performance of the calculation can be improved by increasing the degree of freedom in the model, i.e. by involving diffuse or directional reflection, directional characteristics of the source or the receiver, and so on.

4. Results

Measured impulse responses were band limited to the standard center frequencies from 31.25Hz up to 16kHz and stored as raw floating point data with the sampling rate of 75kHz. From these data using the procedure outlined above, the absorption coefficients of different surfaces were calculated.

Figure 14. shows some measured and predicted ETCs using the new absorption coefficients at low frequencies.

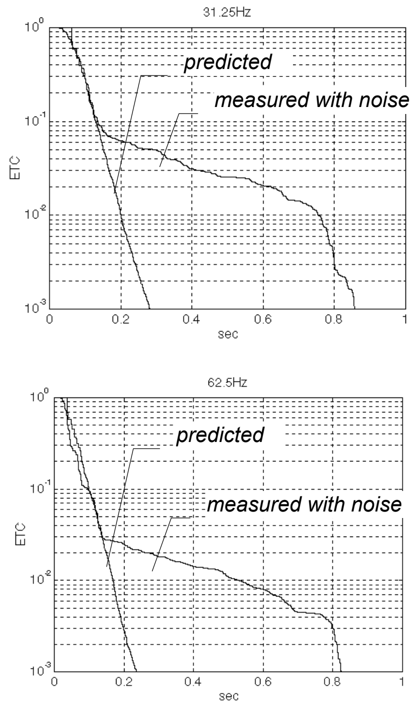

Figure 14. Measured and predicted ETCs with calculated parameters

Some of the calculated absorption coefficients are shown in Fig. 15 with frequency.

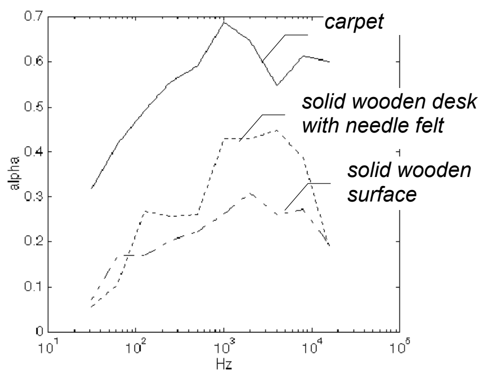

Figure 15. Calculated absorption coefficients

In Fig. 15 the solid line shows the absorption coefficients of surface type 7 (Fig. 13), which was the floor with a wall-to-wall carpet on it. The dashed lines below show absorption coefficients of solid wooden surfaces, where the upper one is a desk coated with needle felt.

5. Conclusions

Although the methods of geometrical room acoustics are only coarse simulations of what really takes place in the sound field of a room, our examinations showed they can be used even in the extreme situation of acoustically treated small rooms.

The accuracy of these algorithms may be significantly improved just by tuning different the parameters. To match the measured ETCs, a new method for estimating the absorption coefficients was presented.

Results, calculated from measurements and predictions at different excitation and receiver points in the same room correlated well. As one would expect, differences occured mainly at surfaces far from the receiver point and at higher frequencies. These errors could be explained here with the very fast decay rate and the directional properties of the sources.

6. Further work

The 'inverse' calculation of absorption coefficients is a promising way for determining the correct parameters. Although these results were developed only for the modeling, it is an interesting task to check their consistency in other situations, too. For example:

- same surface type and room, different position,
- same surface type and room, excited from different positions, and detected in different positions, and finally
- same surface type but in different room.

If the last situation gives the same results as the previous ones, this method could be used also for measurement purposes. The study the influence of diffuse reflections, diffraction, etc. is also necessary.

Based on the idea of utilizing the temporal distribution of reflections to determine their amplitudes and that predicted and measured energy-time curves can be matched almost directly, several other new 'inverse' method could be developed and proved to be reliable in the future.

References

[1] 'Binaurale Raumsimulation: Ein Computermodell zur Erzeugung virtueller auditiver Umgebungen': H. Lehnert - PhD Thesis, Bochum, 1992, (ISBN 3-86111-166-7)

[2] 'Room Acoustics': K. H. Kuttruff - Applied Science Pub., Essex, 1979 (ISBN 0-85334-813-8)

[3] 'Auralization of Impulse Responses Modeled on the Basis of Ray-Tracing Results': K. H. Kuttruff - AES Journal, Vol. 41 No. 11, 1993 November, 876-880

[4] 'New Reference Listening Room for Two-Channel and Multichannel Stereophony': É. Borsi-Arató, A. T. Fürjes, T. Póth - 104th AES Convention Amsterdam, the Netherlands, 1998 May

[5] 'A Macroscopic View of Diffuse Reflection': B-I. Dalenbäck, M. Kleiner, P. Svensson - AES Journal, Vol. 42. 1994, 793-806

[6] 'Noise and Vibration Engineering': ed. L.L. Beranek, I.L Vér - John Wiley, New York, 1992 (ISBN 0-471-61751-2)